ACS Photonics

Open Access

This article is licensed under CC-BY-NC-ND 4.0

pubs.acs.org/journal/apchd5

Letter

On-Demand Generation of Indistinguishable Photons in the Telecom C-Band Using Quantum Dot Devices

Daniel A. Vajner, Paweł Holewa, Emilia Zięba-Ostój, Maja Wasiluk, Martin von Helversen, Aurimas Sakanas, Alexander Huck, Kresten Yvind, Niels Gregersen, Anna Musiał, Marcin Syperek, Elizaveta Semenova, and Tobias Heindel*

Cite This: ACS Photonics 2024, 11, 339−347

Read Online

ACCESS | Metrics & More | Article Recommendations | Supporting Information

ABSTRACT: Semiconductor quantum dots (QDs) enable the generation of single and entangled photons, which are useful for various applications in photonic quantum technologies. Specifically for quantum communication via fiber-optical networks, operation in the telecom C-band centered around 1550 nm is ideal. The direct generation of QD-photons in this spectral range with high quantum-optical quality, however, remained challenging. Here, we demonstrate the coherent on-demand generation of indistinguishable photons in the telecom C-band from single QD devices consisting of InAs/InP QD-mesa structures heterogeneously integrated with a metallic reflector on a silicon wafer. Using pulsed two-photon resonant excitation of the biexciton−exciton radiative cascade, we observe Rabi rotations up to pulse areas of 4π and a high single-photon purity in terms of $g^{(2)}(0)$ = 0.005(1) and 0.015(1) for exciton and biexciton photons, respectively. Applying two independent experimental methods, based on fitting Rabi rotations in the emission intensity and performing photon cross-correlation measurements, we consistently obtain preparation fidelities at the π-pulse exceeding 80%. Finally, performing Hong−Ou−Mandel-type two-photon interference experiments, we obtain a photon-indistinguishability of the full photon wave packet of up to 35(3)%, representing a significant advancement in the photon-indistinguishability of single photons emitted directly in the telecom C-band.

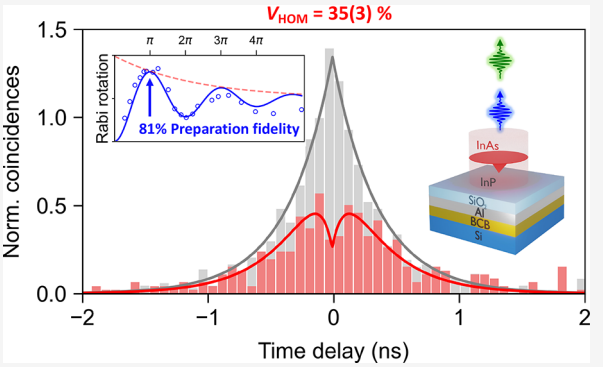

KEYWORDS: *single photon sources, quantum dots, quantum communication, coherent excitation, telecom C-band*

INTRODUCTION

Single indistinguishable photons are a key resource for many applications in quantum information, ranging from quantum communication to distributed quantum computing. They are essential for quantum networks and the quantum internet.[1] While a plethora of quantum emitters enable the generation of single photons,[2,3] epitaxial semiconductor quantum dots (QDs) turned out to be advantageous in many regards.[4−7] Over the last decades, photons generated on-demand using QDs demonstrated unprecedented quantum optical properties in terms of high purity, brightness, and indistinguishability and have been repeatedly employed in implementations of quantum communication.[8] So far, such close-to-ideal single-photon sources have only been demonstrated at wavelengths around 780 nm for GaAs/AlGaAs QDs[9,10] and 930 nm for InGaAs/GaAs QDs.[11−13] For long-distance quantum information transfer via optical fibers, however, wavelengths around 1550 nm, i.e., in the telecom C-band, are required to benefit from the lowest losses in optical fibers. To shift the emission of QDs to C-band wavelengths, quantum frequency conversion of QD-photons emitted at shorter wavelengths can be used,[14,15] which however introduces additional conversion losses, ultimately limiting the source efficiency. For this reason, QDs directly emitting photons at telecom wavelengths are desirable, requiring carefully tailored growth schemes.

One solution is to introduce metamorphic buffer layers to engineer the strain and size of InAs/InGaAs QDs, which shifts the emission to longer wavelengths.[16] QDs for the telecom C-band grown on metamorphic buffers have been advanced in recent years,[17,18] and recently triggered photon-indistinguishabilities of $V \approx 10\%$ and $V = 14(2)\%$ were reported under quasi-resonant[19] and resonant[20] excitation, respectively. An alternative approach uses the InP material system to grow InAs/InP QDs naturally emitting at telecom C-band wavelengths. Here, no additional metamorphic buffer layer is required, which enables the high crystalline quality of the QD

Received: July 11, 2023
Revised: December 22, 2023
Accepted: December 26, 2023
Published: January 23, 2024

© 2024 The Authors. Published by American Chemical Society

material and reduces the complexity of the growth in favor of improved device scalability. Various studies investigated the properties of InP-based QDs under above-barrier and quasi-resonant excitation.[21−26] A notable recent advancement in this context concerns the demonstration of a scalable device platform, by deterministically integrating single InAs/InP QDs into circular Bragg grating cavities, resulting in a triggered, Purcell-enhanced emission and a photon-indistinguishability of V = 19(3)% under quasi-resonant excitation.[27] The pulsed coherent generation of indistinguishable single photons from QDs at C-band wavelengths, however, is an important requirement for applications that had not been achieved to date. Pulsed photon generation is indispensable for on-demand operation, and coherent excitation promises the best single-photon properties, in particular, a high quantum state preparation fidelity, as needed for quantum network applications.

This work presents studies on single InAs/InP QDs integrated into mesa structures and excited via pulsed coherent excitation. Coherently driving the biexciton−exciton (XX-X) radiative cascade via triggered two-photon-resonant excitation (TPE) of the XX-state, we demonstrate the on-demand generation of single photons with high purity in terms of $g^{(2)}(0) \approx 1\%$ and record-high photon-indistinguishabilities of V_{HOM} = 35(3)% in the telecom C-band. Our work thus represents a notable advancement in the generation of flying qubits for quantum networking in optical fibers.

RESULTS AND DISCUSSION

The QD devices (see Figure 1a) used in this work are based on InAs/InP QDs embedded in mesa structures integrated on a bottom metallic mirror (aluminum) to enhance the photon extraction efficiency to ≈10%.[26] Heterogeneous integration on a silicon (Si) carrier thereby allows for future integration in the complementary metal-oxide-semiconductor (CMOS) platform. See the Methods section for details on the device fabrication. Noteworthy in this context, quantum emitter integration on Si has also been demonstrated at O-band wavelengths in the range of 1310−1440 nm.[29−31] Coherent excitation schemes, however, have not yet been implemented on CMOS compatible samples.

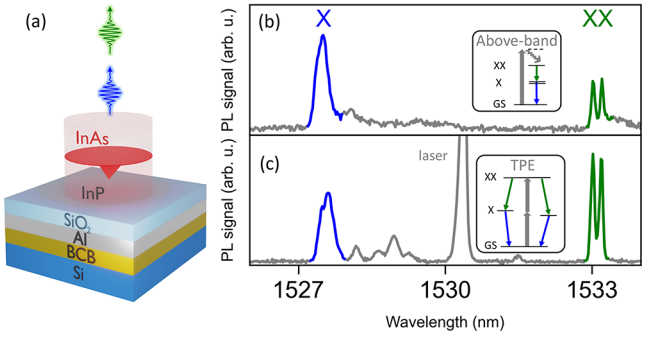

Figure 1. (a) Illustration of the Si-compatible QD-mesa structure used in this study: a single InAs QD is embedded in an InP matrix with a metallic Al bottom mirror for enhanced photon extraction efficiency. The mesa diameter is 2 μm. (b) Spectrum of a QD-mesa under above-barrier excitation at saturation power revealing telecom C-band photons originating from the X- (blue) and XX- (green) radiative recombination, respectively. (c) Spectrum of the same QD under two-photon resonant (TPE) excitation. The center peak originates from residual scattering of the pump laser. Insets illustrate the excitation scheme used. All spectra are taken at 4 K, and the emission is collected via an NA = 0.7 aspheric lens.

The spectrum of a single QD-mesa recorded at 4 K under above-barrier excitation (continuous wave (CW) laser at 980 nm) is shown in Figure 1b. Photons originating from the XX-X radiative cascade are observed with wavelengths near 1530 nm in the telecom C-band. The assignment of the QD states was confirmed via polarization- and excitation-power-dependent photoluminescence measurements, as well as photon cross-correlation experiments (SI, section IB). We observe a fine structure splitting (FSS) of the X state of 88(2) μeV and a binding energy of the XX-state of 2.9(1) meV, allowing for TPE of the biexciton state.[32] Figure 1c depicts a spectrum of the same QD from (b) under pulsed TPE (see Methods for details), revealing the same spectral fingerprint of the QD together with remaining scattered laser light near 1530 nm. We extract upper bounds for the linewidths under TPE of 119(7) μeV and 47(2) μeV fwhm for the X- and XX-transition, respectively (see SI, section IC).

The coherent population of the XX-X cascade under TPE can be confirmed via excitation-power dependent measurements. Figure 2a and b display the laser-power-dependent spectrally filtered photoluminescence signal from the X- and XX-state, respectively, detected using a single-photon detector (see the Methods for details). Here, clear Rabi rotations are observed up to pulse areas of 4π accompanied by a noticeable damping effect. Note that unlike under strictly resonant excitation, the Rabi frequency scales quadratically with the pulse area under TPE, resulting in equidistant Rabi oscillations as a function of the laser power. Note also that in the presence of damping the pulse area that leads to a complete occupation inversion (the theoretical π-power) slightly deviates from the power that leads to a maximum in the detected emission. However, here we denote the maximum of the measured Rabi rotation as the π-power for simplicity.

To estimate the preparation fidelity from the measured Rabi rotations, we follow refs 10 and 18 using an exponentially damped oscillation derived by extending an analytical approximation (see Methods and SI, section IIA, for details). The fit describes the data well up to a pulse area of 4π, while it deviates for higher pulse areas. This deviation can be understood by a quenching of the X and XX emission at high powers as the generation of a high number of excess charges at high power favors the formation of trion states. This hypothesis was confirmed by adding a weak above-barrier CW excitation to the pulsed TPE which reduces the X and XX emission signal while enhancing the trion emission (see SI, section ID for details). By extrapolating the fitted envelope function of the oscillations (dashed red line) one obtains an estimated preparation fidelity, i.e., normalized occupation at π-power, of $\mathcal{F}_{prep}$ = 81(4)% and 82(4)% for X and XX, respectively, which translates into a pair generation fidelity of 66%. This observed preparation fidelity compares favorably or is comparable with previously reported values between 49% and 85% for QDs at C-band wavelength based on metamorphic buffer layers (see also Table 1).[18,36] Note that an alternative approach based on photon cross-correlation experiments will be used further below to independently confirm the preparation fidelities obtained above.

From now on and unless stated otherwise, experiments were conducted under TPE with a π-pulse corresponding to P_π = 2.5 μW average excitation power, measured in front of the cryostat

https://doi.org/10.1021/acsphotonics.3c00973
ACS Photonics 2024, 11, 339−347

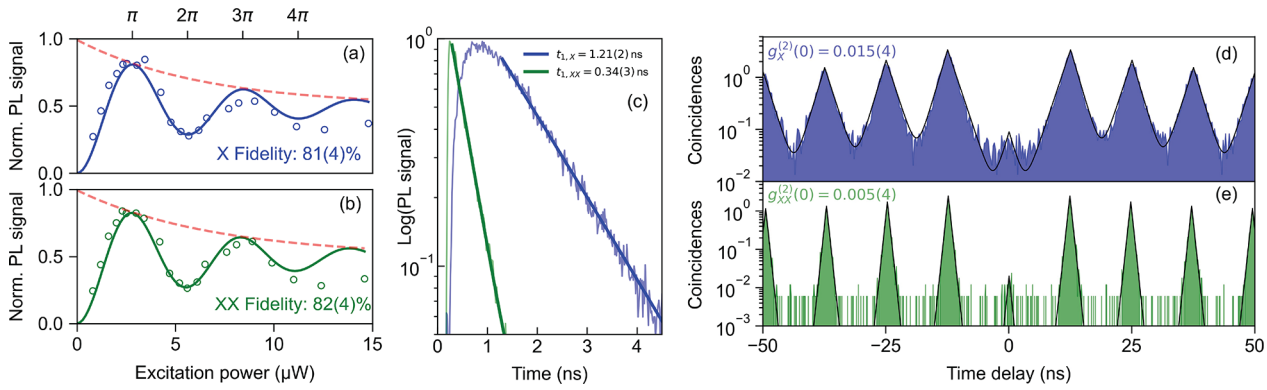

Figure 2. (a, b) Tuning the excitation laser power reveals Rabi rotations in the spectrally filtered single-photon detector counts of the X- (blue, upper panel) and XX- (green, lower panel) states up to 4π, confirming the coherent population of the three-level system. Solid lines correspond to fits and dashed red lines to the extracted envelope function from which preparation fidelities >80% are extracted. (c) The decay dynamics illustrate the cascaded emission under pulsed TPE, with the X-photons (blue line) appearing delayed with respect to the XX-photons (green). The XX-state decays ≈4× faster than the X-state. (d, e) The second-order autocorrelation measurement confirms the single-photon-nature of X- (blue) and XX- (green) emission.

Table 1. Comparison of Reported Pulsed HOM Visibilities V_{HOM} and Preparation Fidelities $\mathcal{F}_{prep}$ for Single Photons Emitted by QDs in the Telecom C-Band[a]

QD type	device	excitation	pulsed V_{HOM}	$\mathcal{F}_{prep}$	ref
InAs/InP	Mesa	TPE	V_{4ns} = 35(3)%	81(2)%	this work
InAs/InP	Mesa	TPE	V_{raw} = 29(2)%	81(2)%	this work
InAs/InP	CBG	QR	V_{4ns} = 19(3)%		Holewa et al. 2023[27]
InAs/InGaAs + MB	CBG	QR	V_{6ns} ≈ 10%		Nawrath et al. 2023[19]
InAs/InGaAs + MB	planar	TPE		84(3)%	Zeuner et al. 2021[18]
InAs/InGaAs + MB	planar	R	V_{4ns} = 14(2)%		Nawrath et al. 2021[20]
InAs/InGaAs + MB	planar	R		49(6)%	Nawrath et al. 2019[36]

[a]MB: Metamorphic buffer layer; CBG: Circular Bragg grating; R: resonant; TPE: two-photon-resonant; QR: quasi-resonant. The subscript of the visibility V refers to the coincidence histogram integration window when evaluating the HOM measurement.

window. To gain insights into the dynamics of the three-level system under study, time-resolved measurements were conducted (see Methods for experimental details). In Figure 2c, we observe the typical behavior of the XX-X emission cascade. A fast exponential decay of the XX-state causes the X state to be transiently occupied, followed by a slower exponential decay of the X-state. Applying monoexponential fits to the time traces, we extract the respective decay constants as

$$t_{1,X} = 1.21(2)\ \text{ns}, \quad t_{1,XX} = 0.34(3)\ \text{ns}$$

Interestingly, the decay of the XX-state is about 4× faster than the decay of the X-state, a characteristic that was also verified for other QDs on the same sample (see SI, section IF). Possible explanations include a specific QD morphology resulting in an increased electron−hole wave function overlap for the XX state[39,40] or additional decay channels via dark exciton states enabled by intrinsically short spin-flip times as discussed in ref 41. To generate polarization entangled photon pairs, the XX-X emission cascade is typically used. For photons originating from the cascaded decay, the indistinguishability is intrinsically limited as the X photons inherit the timing jitter from the XX decay, while the XX photons decay into a spectrally broadened X state. Hence, the achievable indistinguishability is upper bounded by the ratio of the XX- and X-lifetime as $V_{max,TPE} = 1/(1 + t_{1,XX}/t_{1,X})$.[42] This results in a theoretical limit of ≈80% in our case, which significantly exceeds the value of 67% resulting from the often assumed case of $t_{1,X} = 2 \times t_{1,XX}$. Thus, the InAs/InP QDs investigated here, which exhibit a larger $t_{1,X}/t_{1,XX}$ ratio, are promising candidates for combining entanglement generation with high photon indistinguishability. Technologically more involved approaches in this direction aim to exploit microcavities supporting an asymmetric Purcell enhancement for maximizing this lifetime ratio.[43]

Next, we investigated the purity of the single photons in terms of the second-order autocorrelation function $g^{(2)}(\tau)$ via Hanbury−Brown- and Twiss-type experiments. The resulting $g^{(2)}(\tau)$-histograms for X- and XX-photons are presented in Figure 2d and e, respectively. The strong suppression of coincidences at zero time delay confirms the emission of single photons. The experimental data are approximated by a fit function corresponding to a sum of two-sided exponential decays and accounting for the noticeable blinking effect on short time scales, following ref 27 (see SI, section IIIA for details), while no temporal deconvolution or background subtraction was applied. The fit yields antibunching values of

$$g^{(2)}_X(0) = 0.015(4), \quad g^{(2)}_{XX}(0) = 0.005(4)$$

where the errors have been determined from the fit residuals. The decay times obtained from the fit are 1.44(1) and 0.36(1) ns for the X- and XX-state, respectively, in good agreement with the time-resolved photoluminescence measurements. We further extract the time scale of the blinking as $\tau_{blink} \approx 17(1)$ ns, which can be caused by either charging events or spectral wandering due to fluctuation in the QD's charge environment.

https://doi.org/10.1021/acsphotonics.3c00973
ACS Photonics 2024, 11, 339−347

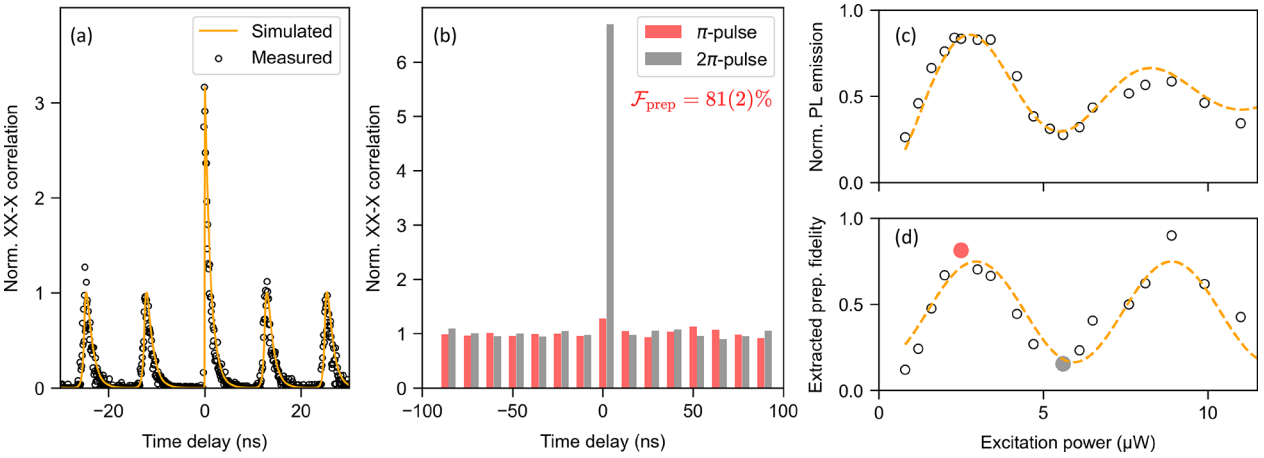

Figure 3. Analysis of the preparation fidelity via XX-X photon cross-correlation experiments: (a) Measured cross-correlation histogram after polarization and blinking correction (grey bars), matching the Monte Carlo simulation (orange line) of expected polarization-filtered XX-X correlation for a QD with a DOP of 33% and a preparation fidelity of 81%. (b) Comparison of polarization-corrected and integrated coincidences at π-power (red) and at 2π-power (gray, shifted for clarity) shows difference in preparation fidelity. (c) Summed XX and X emission intensity oscillation as a function of excitation power with Rabi fit from Figure 2a (orange line) for comparison. (d) Preparation fidelity $\mathcal{F}_{prep}$ extracted from cross-correlation histograms as a function of excitation power. Red and gray circles indicate the data sets shown in panel (b) (orange line is a guide to the eye).

Having confirmed the coherent population of the XX-X cascade via TPE by observing Rabi rotations in Figure 2a,b, revealing a fidelity for preparing the XX- (X-) state of 82(4)% (81(4)%), we applied another independent method for extracting the preparation fidelity to verify our results. For this purpose, photon cross-correlation experiments between photons emitted from the XX- and X-state were carried out[44] (see Methods and SI, section IIA for details). Figure 3a depicts the photon cross-correlation histogram recorded at π-pulse excitation (black circles) together with a Monte Carlo simulation (orange line) accounting for our experimental conditions (including setup imperfections). The experimental data, obtained under TPE at π-power and corrected for polarization and blinking effects as mentioned above, are consistent with a preparation fidelity of 81%. The simulations are in very good agreement and also reproduce fine details, such as the correct area ratios, the asymmetry of the side peaks caused by the faster XX decay, and the strong asymmetry in the center peak caused by the cascaded decay (see SI, section IIB for details on simulation). The comparison of the integrated coincidence-peak areas depicted in Figure 3b yields a maximum preparation fidelity of 81(2)% at π-power (red bars) in perfect agreement with the value determined from the Rabi rotation in the emission intensities in Figure 2a,b. The error is determined from the standard deviation of the noncenter peak areas. At 2π-power (gray bars) the preparation fidelity reduces to 14(2)%. Complementary data under off-resonant excitation (see SI, Section IIA) yielded a preparation fidelity of 44(2)%), clearly confirming the positive impact of coherent excitation. By extracting the preparation fidelity from the cross-correlation experiments as a function of the excitation power (cf. Figure 3d), oscillations of the preparation fidelity can be observed which are in phase with the Rabi rotations of the emission (cf. Figure 3c). Interestingly, the fidelity oscillations do not exhibit the same damping observed in the Rabi rotations.

Finally, we explored the indistinguishability of the XX-photons emitted by the coherently driven three-level system via Hong−Ou−Mandel (HOM)-type two-photon interference experiments (see Methods for details). The resulting experimental data for the co- and cross-polarized measurement configuration are presented in Figure 4 as a close-up

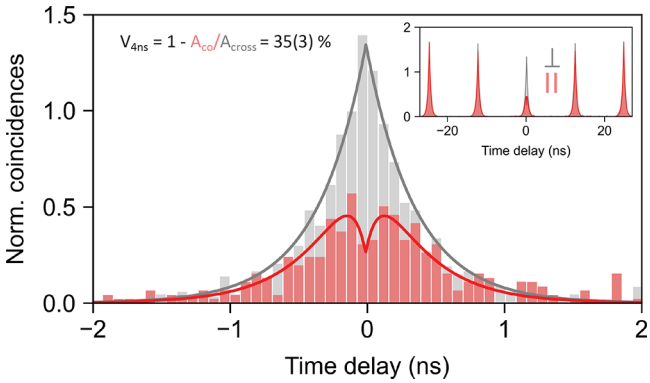

Figure 4. HOM-type two-photon interference experiments of photons emitted by the XX-state for co- (red) and cross- (gray) polarized measurement configuration. Photon coalescence described by the Hong−Ou−Mandel effect is confirmed by the clear suppression of coincidences in the central peak for copolarized photons. We observe record-high photon-indistinguishabilities of V_{raw} = 29(2)% and V_{4ns} = 35(3)% by integrating the raw experimental data over the full 12.5 ns- and a 4 ns-wide delay-window, respectively. The inset shows the same data for a broader range of arrival time delays.

highlighting the zero-delay peak. The reduction of coincidences due to two-photon interference is clearly visible. Additionally, the inset depicts the histograms for larger arrival time delays. Note that the ratios of the coincidence side-peak areas deviate from the expected behavior as they are masked by the blinking effect. This, however, does not affect the following analysis, which is solely based on the integrated zero-delay peak areas for co- and cross-polarized measurements (without applying the fit model).

The two-photon interference visibility is extracted from our measurement data via $V_{HOM} = 1 - (A_{co}/A_{cross})$, with the integrated areas A_{co} and A_{cross} of the copolarized and cross-

https://doi.org/10.1021/acsphotonics.3c00973
ACS Photonics 2024, 11, 339−347

polarized case, respectively. Integrating over the entire zero-delay time window, i.e., −6.25 to +6.25 ns (corresponding to the laser repetition rate of 80 MHz), yields V_{raw} = 29(2)%, with the error inferred from the distribution of the integrated detection events of the noninterfering side peaks. This photon-indistinguishability readily exceeds all previous reports on pulsed HOM experiments of telecom C-band photons directly generated via QDs (cf. Table 1), including pioneering work by Nawrath et al.,[19,20] as well as our most recent work in ref 27.

Note that in these earlier reports, typically photons with a temporal separation of 4 ns were interfered. Thus, for the sake of comparison, we also evaluate the two-photon interference visibility for a 4 ns-wide integration window as V_{4ns} = 35(3)%. Importantly, this integration window covers over 99% of all coincidences detected in the zero-delay peak. Thus, the increase of V_{4ns} compared to V_{raw} results from the improved signal-to-noise ratio (due to reduced noise contributions by dark counts) rather than discarding signal events. In addition, by interfering photons with a temporal separation of 12.5 ns, the QD-excitonic states investigated in our work are potentially subject to larger dephasing compared to previous studies that used Δt = 4 ns.[46]

While the photon-indistinguishability observed in our work represents a substantial improvement compared to previous reports on QD photons emitted directly at C-band wavelengths, it is not yet competitive with up-converted photons from QDs emitting at lower wavelengths.[15] As the achieved indistinguishability is well below the limit of 80% set by the ratio of the measured radiative lifetimes,[42] there are still other limiting factors. The main contribution currently limiting the photon-indistinguishability is suspected to be charge fluctuations in the QD environment, as evidenced by a considerable blinking effect in the autocorrelation measurement, the presence of a predominant trion state under above-barrier excitation, as well as the influence of additional weak CW above-barrier excitation during TPE (cf. SI, section ID), which reduces the coherence time of the QD under study. We anticipate two routes to overcome these limitations. First, implementing measures to influence or tailor the electric-field environment of the quantum emitters, using charge stabilization via electrical gates[47,48] or interface passivation.[13] Second, employing droplet-epitaxy,[49] which is known to increase the coherence time,[25] rather than self-assembled Stranski-Krastanov growth of QDs as used in our work. Both routes have independently shown to improve the coherence properties of specific QD systems.

Note for completeness that by performing a fit which includes the central dip (solid lines in Figure 4) and accounting for the blinking effect (see SI, section IIIB for details), one can extract the postselected HOM visibility which amounts to 73(6)% and thus compares well with previous works performing CW HOM experiments on similar QDs.[18,50] One should emphasize that the pulsed HOM result presented above is the most relevant one for applications in quantum information, as it describes the interference of the full photon-wave packets. The coherent on-demand generation of indistinguishable photons via TPE at telecom C-band wavelength achieved in our work represents a significant advance toward applications of quantum information and long-haul quantum communication in optical fibers. Yet, the most suitable excitation scheme for implementations of quantum communication needs to be carefully selected depending on the specific use-case. For defining time bins and synchronizing sender and receiver units, pulsed excitation is needed, while coherent excitation provides the highest photon indistinguishability. Among all known approaches for pumping QD emitters, coherently driving the XX-X cascade via TPE promises the highest purity in terms of $g^{(2)}(0)$, as it reduces the re-excitation probability.[12] In addition, the spectrally detuned excitation laser allows for straightforward spectral filtering of the emitted photons and for the generation of polarization-entangled photon pairs.[51] While the maximum indistinguishability is limited in standard TPE,[42] it can be further boosted by stimulating the XX-decay channel to distill highly indistinguishable X-photons.[52]

Another important aspect in quantum communication concerns whether the emitted photons form a pure or a mixed state in the photon number basis, which strongly depends on the excitation scheme.[53] For most quantum communication protocols, the absence of photon number coherence (PNC) is required to avoid side-channel attacks and maintain security. As recently demonstrated for QD-generated photons at shorter wavelengths, standard TPE does not result in a significant degree of PNC in the emitted photon states, which can however be recovered and tuned by stimulating the XX-decay channel with a second laser pulse.[54]

CONCLUSION

In summary, we demonstrated the pulsed coherent excitation of InAs/InP QDs emitting photons at telecom C-band wavelengths with unprecedented photon-indistinguishability. Using triggered TPE of the XX-X radiative cascade, we coherently populate the three-level system, which is confirmed by the observation of Rabi rotations up to 4π consistently, yielding preparation fidelities exceeding 80%, as confirmed by two independent experimental approaches. The observed two-photon-interference visibility of up to 35(3)% clearly surpasses previous results obtained for triggered photons in the telecom C-band directly emitted by QDs. The type of QDs studied in our work exhibits a large ratio of exciton-to-biexciton lifetime, making them promising candidates for the generation of polarization-entangled photon-pairs with high photon-indistinguishability at the C-band wavelength. The demonstrated on-demand generation of QD photons with record-high indistinguishability at wavelengths compatible with existing fiber infrastructure presents a significant step toward scalable quantum networks.

METHODS

QD Device. The QD devices used in this work are based on InAs/InP QDs obtained via self-assembled Stranski−Krastanow growth in the near-critical regime via metalorganic vapor phase epitaxy (MOVPE).[28] To enhance the photon extraction efficiency, mesa structures are combined with a bottom metallic mirror (aluminum), while bonding via benzocyclobutene (BCB) to the Si-carrier allows for future integration in the CMOS platform. For details on the device fabrication and basic characterization, we refer the interested reader to the Supporting Information (SI), sections IA and IB, as well as ref 26.

Quantum Optics Experiments. The QD devices are investigated by means of low-temperature (4 K) micro-photoluminescence spectroscopy. Samples are mounted inside a closed-cycle an optical table integrated in a cryosphere table (model attoDRY800, attocube systems AG). An aspheric lens

https://doi.org/10.1021/acsphotonics.3c00973
ACS Photonics 2024, 11, 339−347

with an NA of 0.7 inside the cryostat is used to collect the QD emission. For optically pumping single QDs, we use a 980 nm CW laser or a spectrally shaped wavelength-tunable 2.5 ps pulsed laser system (picoEmerald, APE GmbH) with 80 MHz repetition rate. For TPE the picosecond laser is combined with a folded 4f pulse-shaper, resulting in a spectral width of ≈0.5 nm full-width at half-maximum (fwhm) and a stretched pulse duration of 10 ps fwhm. Photons originating from the X- or XX-state are spectrally analyzed using a grating spectrometer (900 grooves/mm) with an attached InGaAs array detector. For time-correlated single-photon counting experiments, the X- and XX-photons are spectrally filtered using a tunable fiber-band-pass filter of 0.4 nm bandwidth in combination with polarization suppression of the scattered excitation laser. Time-resolved measurements were conducted using a superconducting nanowire single photon detector (SNSPD; SingleQuantum EOS, SingleQuantum BV) in combination with time-tagging electronics (quTag, quTools GmbH), with a combined timing resolution of ≈50 ps fwhm.

To measure the purity, we performed Hanbury−Brown and Twiss autocorrelation experiments by passing the spectrally filtered single photons through a 50:50 fiber beamsplitter and registering the arrival time difference between the detectors at the two outputs.

The photon-indistinguishability is measured in HOM-type experiments using a Mach−Zehnder interferometer with a 12.5 ns delay, compensating for the photon delay imposed by the 80 MHz excitation laser. Here, interfering indistinguishable photons cause coalescence in the two interferometer output ports, thus reducing the number of detected coincidences. Additionally, the polarization state of the interfering photons is controlled in both arms of the interferometer, allowing for measurements in co- and cross-polarized configuration, whereas the latter serves as a reference to extract the two-photon-interference visibility V. Here, the visibility was extracted by integrating all coincidences within one excitation cycle for the co- and cross-polarized measurement as well as by selecting a realistic 4 ns time window. For details concerning the data analysis of the time-resolved experiments, we refer to SI, sections IIIA and IIIB.

Estimating Preparation Fidelities. Different approaches can be used to estimate the preparation fidelity. From the Rabi rotations in emission intensity vs excitation power this is possible, e.g., by comparing the occupation at π and 2π power,[33] fitting exponentially damped $\sin^2$ functions,[34] solving rate equation models numerically,[35,36] or by modeling the full system via polaron-transformed open system master equations[37] or correlation expansion approaches to include phonons.[38] To independently confirm the preparation fidelities obtained in our work, we used two different experimental approaches.

In the first approach, used in Figure 2a,b, we model the experimental Rabi data following refs 10 and 18, fitting the experimental Rabi data using an exponentially damped oscillation derived by extending an analytical approximation for CW Rabi oscillations to Rabi rotations in the pulsed regime.

The second approach, used in Figure 3b, is based on photon cross-correlation experiments between photons emitted from the XX- and X-state.[44] Comparing the integrated coincidences originating from the same cascade A_{same} with those from different cascades $A_{\mathrm{different}}$, the preparation fidelity can in principle be extracted as $\mathcal{F}_{\mathrm{prep}} = A_{\mathrm{different}}/A_{\mathrm{same}}$.[45] Importantly, the experimental data had to be corrected to account for partial polarization of the QD emission, the polarization-selective detection in our setup, and the blinking effect discussed above.

For details on the analysis and the required corrections, we refer to the SI, section IIA.

■ ASSOCIATED CONTENT

Supporting Information

The Supporting Information is available free of charge at https://pubs.acs.org/doi/10.1021/acsphotonics.3c00973.

Details on sample fabrication; Identification of excitonic complexes; Additional data on other QDs; Information on lifetime, Rabi, purity, and indistinguishability data evaluation; Extraction of preparation fidelity from Rabi fit and cross-correlation measurements; Simulation of XX-X cascade (PDF)

■ AUTHOR INFORMATION

Corresponding Author

Tobias Heindel − *Institute of Solid State Physics, Technical University of Berlin, 10623 Berlin, Germany;* orcid.org/0000-0003-1148-404X; Email: tobias.heindel@tu-berlin.de

Authors

Daniel A. Vajner − *Institute of Solid State Physics, Technical University of Berlin, 10623 Berlin, Germany;* orcid.org/0000-0002-4900-0277

Paweł Holewa − *Department of Experimental Physics, Faculty of Fundamental Problems of Technology, Wrocław University of Science and Technology, 50-370 Wrocław, Poland; DTU Electro, Department of Electrical and Photonics Engineering, Technical University of Denmark, Kongens Lyngby 2800, Denmark; NanoPhoton − Center for Nanophotonics, Technical University of Denmark, 2800 Kongens Lyngby, Denmark;* orcid.org/0000-0002-2154-896X

Emilia Zięba-Ostój − *Department of Experimental Physics, Faculty of Fundamental Problems of Technology, Wrocław University of Science and Technology, 50-370 Wrocław, Poland;* orcid.org/0000-0001-8083-810X

Maja Wasiluk − *Department of Experimental Physics, Faculty of Fundamental Problems of Technology, Wrocław University of Science and Technology, 50-370 Wrocław, Poland*

Martin von Helversen − *Institute of Solid State Physics, Technical University of Berlin, 10623 Berlin, Germany*

Aurimas Sakanas − *DTU Electro, Department of Electrical and Photonics Engineering, Technical University of Denmark, Kongens Lyngby 2800, Denmark;* orcid.org/0000-0001-5155-5557

Alexander Huck − *Center for Macroscopic Quantum States (bigQ), Department of Physics, Technical University of Denmark, 2800 Kongens Lyngby, Denmark;* orcid.org/0000-0002-2354-5922

Kresten Yvind − *DTU Electro, Department of Electrical and Photonics Engineering, Technical University of Denmark, Kongens Lyngby 2800, Denmark; NanoPhoton − Center for Nanophotonics, Technical University of Denmark, 2800 Kongens Lyngby, Denmark;* orcid.org/0000-0001-8013-1606

Niels Gregersen − *DTU Electro, Department of Electrical and Photonics Engineering, Technical University of Denmark,*

Kongens Lyngby 2800, Denmark; orcid.org/0000-0002-8252-8989

Anna Musiał − *Department of Experimental Physics, Faculty of Fundamental Problems of Technology, Wrocław University of Science and Technology, 50-370 Wrocław, Poland;* orcid.org/0000-0001-9602-8929

Marcin Syperek − *Department of Experimental Physics, Faculty of Fundamental Problems of Technology, Wrocław University of Science and Technology, 50-370 Wrocław, Poland;* orcid.org/0000-0002-5260-7360

Elizaveta Semenova − *DTU Electro, Department of Electrical and Photonics Engineering, Technical University of Denmark, Kongens Lyngby 2800, Denmark; NanoPhoton − Center for Nanophotonics, Technical University of Denmark, 2800 Kongens Lyngby, Denmark;* orcid.org/0000-0002-5856-4461

Complete contact information is available at: https://pubs.acs.org/10.1021/acsphotonics.3c00973

Author Contributions

The concept of the QD device was suggested by E.S. and realized under her supervision at DTU. Epitaxy and nanofabrication was performed by P.H. with support of A.S. and K.Y. The sample design was supported by simulations performed by N.G. Initial optical characterization of the sample was performed in Wrocław by P.H. with support of E.Z., M.W., and A.M. and supervised by M.S. A.H. contributed to the data analysis. The experiments, simulations, and data analysis in this work were conducted in Berlin by D.A.V. under the supervision of T.H. and M.v.H. The manuscript was written by D.A.V., T.H., and M.v.H. with input from all authors. T.H. supervised all efforts in this project.

Funding

We acknowledge financial support by the German Federal Ministry of Education and Research (BMBF) via the project "QuSecure" (Grant No. 13N14876) within the funding program Photonic Research Germany, the BMBF joint project "tubLAN Q.0" (Grant No. 16KISQ087K), the Einstein Foundation via the Einstein Research Unit "Quantum Devices", the Danish National Research Foundation via the Research Centers of Excellence NanoPhoton (DNRF147), and the Center for Macroscopic Quantum States bigQ (DNRF142). P.H. was funded by the Polish National Science Center within the Etiuda 8 scholarship (Grant No. 2020/36/T/ST5/00511). N.G. acknowledges support from the European Research Council (ERC-CoG "UNITY", Grant No. 865230), and from the Independent Research Fund Denmark (Grant No. DFF-9041-00046B).

Notes

The authors declare no competing financial interest.

■ ACKNOWLEDGMENTS

The authors gratefully acknowledge helpful discussions with Yusuf Karli, Florian Kappe, Thomas Bracht, and Doris Reiter.

■ REFERENCES

(1) Kimble, H. J. The quantum internet. *Nature* **2008**, *453*, 1023−1030.

(2) Aharonovich, I.; Englund, D.; Toth, M. Solid-state single-photon emitters. *Nat. Photonics* **2016**, *10*, 631−641.

(3) Chakraborty, C.; Vamivakas, N.; Englund, D. Advances in quantum light emission from 2D materials. *Nanophotonics* **2019**, *8*, 2017−2032.

(4) Senellart, P.; Solomon, G.; White, A. High-performance semiconductor quantum-dot single-photon sources. *Nat. Nanotechnol.* **2017**, *12*, 1026−1039.

(5) Arakawa, Y.; Holmes, M. J. Progress in quantum-dot single photon sources for quantum information technologies: A broad spectrum overview. *Appl. Phys. Rev.* **2020**, *7*, 021309.

(6) Rodt, S.; Reitzenstein, S.; Heindel, T. Deterministically fabricated solid-state quantum-light sources. *J. Phys.: Condens. Matter* **2020**, *32*, 153003.

(7) Lu, C.-Y.; Pan, J.-W. Quantum-dot single-photon sources for the quantum internet. *Nat. Nanotechnol.* **2021**, *16*, 1294−1296.

(8) Vajner, D. A.; Rickert, L.; Gao, T.; Kaymazlar, K.; Heindel, T. Quantum communication using semiconductor quantum dots. *Adv. Quantum Technol.* **2022**, *5*, 2100116.

(9) Schweickert, L.; Jons, K. D.; Zeuner, K. D.; Covre da Silva, S. F.; Huang, H.; Lettner, T.; Reindl, M.; Zichi, J.; Trotta, R.; Rastelli, A.; Zwiller, V. On-demand generation of background-free single photons from a solid-state source. *Appl. Phys. Lett.* **2018**, *112*, 093106.

(10) Schöll, E.; Hanschke, L.; Schweickert, L.; Zeuner, K. D.; Reindl, M.; Covre da Silva, S. F.; Lettner, T.; Trotta, R.; Finley, J. J.; Müller, K.; et al. Resonance fluorescence of GaAs quantum dots with near-unity photon indistinguishability. *Nano Lett.* **2019**, *19*, 2404−2410.

(11) Wang, H.; Duan, Z.-C.; Li, Y.-H.; Chen, S.; Li, J.-P.; He, Y.-M.; Chen, M.-C.; He, Y.; Ding, X.; Peng, C.-Z.; et al. Near-transform-limited single photons from an efficient solid-state quantum emitter. *Phys. Rev. Lett.* **2016**, *116*, 213601.

(12) Hanschke, L.; Fischer, K. A.; Appel, S.; Lukin, D.; Wierzbowski, J.; Sun, S.; Trivedi, R.; Vučković, J.; Finley, J. J.; Müller, K. Quantum dot single-photon sources with ultra-low multi-photon probability. *npj Quantum Inf.* **2018**, *4*, 43.

(13) Tomm, N.; Javadi, A.; Antoniadis, N. O.; Najer, D.; Löbl, M. C.; Korsch, A. R.; Schott, R.; Valentin, S. R.; Wieck, A. D.; Ludwig, A.; et al. A bright and fast source of coherent single photons. *Nat. Nanotechnol.* **2021**, *16*, 399−403.

(14) Kambs, B.; Kettler, J.; Bock, M.; Becker, J. N.; Arend, C.; Lenhard, A.; Portalupi, S. L.; Jetter, M.; Michler, P.; Becher, C. Low-noise quantum frequency down-conversion of indistinguishable photons. *Opt. Express* **2016**, *24*, 22250−22260.

(15) Da Lio, B.; Faurby, C.; Zhou, X.; Chan, M. L.; Uppu, R.; Thyrrestrup, H.; Scholz, S.; Wieck, A. D.; Ludwig, A.; Lodahl, P.; Midolo, L. A Pure and Indistinguishable Single-Photon Source at Telecommunication Wavelength. *Adv. Quantum Technol.* **2022**, *5*, 2200006.

(16) Semenova, E.; Hostein, R.; Patriarche, G.; Mauguin, O.; Largeau, L.; Robert-Philip, I.; Beveratos, A.; Lemaître, A. Metamorphic approach to single quantum dot emission at 1.55 μ m on GaAs substrate. *J. Appl. Phys.* **2008**, *103*, 103533.

(17) Portalupi, S. L.; Jetter, M.; Michler, P. InAs quantum dots grown on metamorphic buffers as non-classical light sources at telecom C-band: A review. *Semicond. Sci. Technol.* **2019**, *34*, 053001.

(18) Zeuner, K. D.; Jöns, K. D.; Schweickert, L.; Reuterskiöld Hedlund, C.; Nuñez Lobato, C.; Lettner, T.; Wang, K.; Gyger, S.; Schöll, E.; Steinhauer, S.; Hammar, M.; Zwiller, V. On-Demand Generation of Entangled Photon Pairs in the Telecom C-Band with InAs Quantum Dots. *ACS Photonics* **2021**, *8*, 2337−2344.

(19) Nawrath, C.; Joos, R.; Kolatschek, S.; Bauer, S.; Pruy, P.; Hornung, F.; Fischer, J.; Huang, J.; Vijayan, P.; Sittig, R.; et al. Bright Source of Purcell-Enhanced, Triggered, Single Photons in the Telecom C-Band. *Adv. Quantum Technol.* **2023**, *6*, 2300111.

(20) Nawrath, C.; Vural, H.; Fischer, J.; Schaber, R.; Portalupi, S.; Jetter, M.; Michler, P. Resonance fluorescence of single In (Ga) As quantum dots emitting in the telecom C-band. *Appl. Phys. Lett.* **2021**, *118*, 244002.

(21) Birowosuto, M. D.; Sumikura, H.; Matsuo, S.; Taniyama, H.; van Veldhoven, P. J.; Nötzel, R.; Notomi, M. Fast Purcell-enhanced

single photon source in 1,550-nm telecom band from a resonant quantum dot-cavity coupling. *Sci. Rep.* **2012**, *2*, 321.
(22) Miyazawa, T.; Takemoto, K.; Nambu, Y.; Miki, S.; Yamashita, T.; Terai, H.; Fujiwara, M.; Sasaki, M.; Sakuma, Y.; Takatsu, M.; et al. Single-photon emission at 1.5 μm from an InAs/InP quantum dot with highly suppressed multi-photon emission probabilities. *Appl. Phys. Lett.* **2016**, *109*, 132106.
(23) Müller, T.; Skiba-Szymanska, J.; Krysa, A.; Huwer, J.; Felle, M.; Anderson, M.; Stevenson, R.; Heffernan, J.; Ritchie, D. A.; Shields, A. A quantum light-emitting diode for the standard telecom window around 1550 nm. *Nat. Commun.* **2018**, *9*, 862.
(24) Musiał, A.; Mikulicz, M.; Mrowiński, P.; Zielińska, A.; Sitarek, P.; Wyborski, P.; Kuniej, M.; Reithmaier, J.; Sęk, G.; Benyoucef, M. InP-based single-photon sources operating at telecom C-band with increased extraction efficiency. *Appl. Phys. Lett.* **2021**, *118*, 221101.
(25) Anderson, M.; Müller, T.; Skiba-Szymanska, J.; Krysa, A.; Huwer, J.; Stevenson, R.; Heffernan, J.; Ritchie, D.; Shields, A. Coherence in single photon emission from droplet epitaxy and Stranski−Krastanov quantum dots in the telecom C-band. *Appl. Phys. Lett.* **2021**, *118*, 014003.
(26) Holewa, P.; Sakanas, A.; Gür, U. M.; Mrowiński, P.; Huck, A.; Wang, B.-Y.; Musiał, A.; Yvind, K.; Gregersen, N.; Syperek, M.; et al. Bright quantum dot single-photon emitters at telecom bands heterogeneously integrated on Si. *ACS Photonics* **2022**, *9*, 2273−2279.
(27) Holewa, P.; Zięba-Ostój, E.; Vajner, D. A.; Wasiluk, M.; Gaál, B.; Sakanas, A.; Burakowski, M.; Mrowiński, P.; Krajnik, B.; Xiong, M. Scalable quantum photonic devices emitting indistinguishable photons in the telecom C-band. *arXiv:2304.02515 [quant-ph]* **2023**, na.
(28) Berdnikov, Y.; Holewa, P.; Kadkhodazadeh, S.; Smigiel, J. M.; Frackowiak, A.; Sakanas, A.; Yvind, K.; Syperek, M.; Semenova, E. Fine-tunable near-critical Stranski-Krastanov growth of InAs/InP quantum dots. *arXiv:2301.11008 [cond-mat.mes-hall]* **2023**, (accessed 05-01-2024).
(29) Kim, J.-H.; Aghaeimeibodi, S.; Richardson, C. J.; Leavitt, R. P.; Englund, D.; Waks, E. Hybrid integration of solid-state quantum emitters on a silicon photonic chip. *Nano Lett.* **2017**, *17*, 7394−7400.
(30) Katsumi, R.; Ota, Y.; Tajiri, T.; Iwamoto, S.; Ranbir, K.; Reithmaier, J. P.; Benyoucef, M.; Arakawa, Y. CMOS-compatible integration of telecom band InAs/InP quantum-dot single-photon sources on a Si chip using transfer printing. *App. Phys. Express* **2023**, *16*, 012004.
(31) Larocque, H.; Buyukkaya, M. A.; Errando-Herranz, C.; Harper, S.; Carolan, J.; Lee, C.-M.; Richardson, C. J.; Leake, G. L.; Coleman, D. J.; Fanto, M. L. Tunable quantum emitters on large-scale foundry silicon photonics. *arXiv:2306.06460 [physics.optics]* **2023**, (accessed 05-01-2024).
(32) Jayakumar, H.; Predojević, A.; Huber, T.; Kauten, T.; Solomon, G. S.; Weihs, G. Deterministic photon pairs and coherent optical control of a single quantum dot. *Phys. Rev. Lett.* **2013**, *110*, 135505.
(33) Müller, M.; Bounouar, S.; Jöns, K. D.; Glässl, M.; Michler, P. On-demand generation of indistinguishable polarization-entangled photon pairs. *Nat. Photonics* **2014**, *8*, 224−228.
(34) Reindl, M.; Huber, D.; Schimpf, C.; da Silva, S. F. C.; Rota, M. B.; Huang, H.; Zwiller, V.; Jöns, K. D.; Rastelli, A.; Trotta, R. All-photonic quantum teleportation using on-demand solid-state quantum emitters. *Sci. Adv.* **2018**, *4*, No. eaau1255.
(35) Wang, Q.; Muller, A.; Bianucci, P.; Rossi, E.; Xue, Q.; Takagahara, T.; Piermarocchi, C.; MacDonald, A.; Shih, C. Decoherence processes during optical manipulation of excitonic qubits in semiconductor quantum dots. *Phys. Rev. B* **2005**, *72*, 035306.
(36) Nawrath, C.; Olbrich, F.; Paul, M.; Portalupi, S.; Jetter, M.; Michler, P. Coherence and indistinguishability of highly pure single photons from non-resonantly and resonantly excited telecom C-band quantum dots. *Appl. Phys. Lett.* **2019**, *115*, 023103.
(37) McCutcheon, D. P.; Dattani, N. S.; Gauger, E. M.; Lovett, B. W.; Nazir, A. A general approach to quantum dynamics using a variational master equation: Application to phonon-damped Rabi rotations in quantum dots. *Phys. Rev. B* **2011**, *84*, 081305.
(38) Krügel, A.; Axt, V. M.; Kuhn, T.; Machnikowski, P.; Vagov, A. The role of acoustic phonons for Rabi oscillations in semiconductor quantum dots. *Appl. Phys. B: Laser Opt.* **2005**, *81*, 897−904.
(39) Bacher, G.; Weigand, R.; Seufert, J.; Kulakovskii, V.; Gippius, N.; Forchel, A.; Leonardi, K.; Hommel, D. Biexciton versus exciton lifetime in a single semiconductor quantum dot. *Phys. Rev. Lett.* **1999**, *83*, 4417.
(40) Baier, M.; Malko, A.; Pelucchi, E.; Oberli, D.; Kapon, E. Quantum-dot exciton dynamics probed by photon-correlation spectroscopy. *Phys. Rev. B* **2006**, *73*, 205321.
(41) Narvaez, G. A.; Bester, G.; Franceschetti, A.; Zunger, A. Excitonic exchange effects on the radiative decay time of monoexcitons and biexcitons in quantum dots. *Phys. Rev. B* **2006**, *74*, 205422.
(42) Schöll, E.; Schweickert, L.; Hanschke, L.; Zeuner, K. D.; Sbresny, F.; Lettner, T.; Trivedi, R.; Reindl, M.; Da Silva, S. F. C.; Trotta, R.; et al. Crux of using the cascaded emission of a three-level quantum ladder system to generate indistinguishable photons. *Phys. Rev. Lett.* **2020**, *125*, 233605.
(43) Bauch, D.; Siebert, D.; Jöns, K. D.; Förstner, J.; Schumacher, S. On-demand indistinguishable and entangled photons at telecom frequencies using tailored cavity designs. *arXiv:2303.13871 [quant-ph]* **2023**, (accessed 05-01-2024).
(44) Neuwirth, J.; Basset, F. B.; Rota, M. B.; Hartel, J.-G.; Sartison, M.; da Silva, S. F. C.; Jöns, K. D.; Rastelli, A.; Trotta, R. Multipair-free source of entangled photons in the solid state. *Phys. Rev. B* **2022**, *106*, L241402.
(45) Wang, H.; Hu, H.; Chung, T.-H.; Qin, J.; Yang, X.; Li, J.-P.; Liu, R.-Z.; Zhong, H.-S.; He, Y.-M.; Ding, X.; et al. On-demand semiconductor source of entangled photons which simultaneously has high fidelity, efficiency, and indistinguishability. *Phys. Rev. Lett.* **2019**, *122*, 113602.
(46) Thoma, A.; Schnauber, P.; Gschrey, M.; Seifried, M.; Wolters, J.; Schulze, J.-H.; Strittmatter, A.; Rodt, S.; Carmele, A.; Knorr, A.; et al. Exploring dephasing of a solid-state quantum emitter via time- and temperature-dependent Hong-Ou-Mandel experiments. *Phys. Rev. Lett.* **2016**, *116*, 033601.
(47) Somaschi, N.; Giesz, V.; De Santis, L.; Loredo, J.; Almeida, M. P.; Hornecker, G.; Portalupi, S. L.; Grange, T.; Anton, C.; Demory, J.; et al. Near-optimal single-photon sources in the solid state. *Nat. Photonics* **2016**, *10*, 340−345.
(48) Zhai, L.; Löbl, M. C.; Nguyen, G. N.; Ritzmann, J.; Javadi, A.; Spinnler, C.; Wieck, A. D.; Ludwig, A.; Warburton, R. J. Low-noise GaAs quantum dots for quantum photonics. *Nat. Commun.* **2020**, *11*, 4745.
(49) Holewa, P.; Kadkhodazadeh, S.; Gawełczyk, M.; Baluta, P.; Musiał, A.; Dubrovskii, V. G.; Syperek, M.; Semenova, E. Droplet epitaxy symmetric InAs/InP quantum dots for quantum emission in the third telecom window: morphology, optical and electronic properties. *Nanophotonics* **2022**, *11*, 1515−1526.
(50) Anderson, M.; Müller, T.; Huwer, J.; Skiba-Szymanska, J.; Krysa, A.; Stevenson, R.; Heffernan, J.; Ritchie, D.; Shields, A. Quantum teleportation using highly coherent emission from telecom C-band quantum dots. *npj Quantum Inf.* **2020**, *6*, 14.
(51) Huber, D.; Reindl, M.; Aberl, J.; Rastelli, A.; Trotta, R. Semiconductor quantum dots as an ideal source of polarization-entangled photon pairs on-demand: a review. *J. Opt.* **2018**, *20*, 073002.
(52) Wei, Y.; Liu, S.; Li, X.; Yu, Y.; Su, X.; Li, S.; Shang, X.; Liu, H.; Hao, H.; Ni, H.; Yu, S.; Niu, Z.; Iles-Smith, J.; Liu, J.; Wang, X. Tailoring solid-state single-photon sources with stimulated emissions. *Nat. Nanotechnol.* **2022**, *17*, 470−476.
(53) Bozzio, M.; Vyvlecka, M.; Cosacchi, M.; Nawrath, C.; Seidelmann, T.; Loredo, J. C.; Portalupi, S. L.; Axt, V. M.; Michler, P.; Walther, P. Enhancing quantum cryptography with quantum dot single-photon sources. *npj Quantum Inf.* **2022**, *8*, 104.

https://doi.org/10.1021/acsphotonics.3c00973
ACS Photonics 2024, 11, 339−347

(54) Karli, Y.; Vajner, D. A.; Kappe, F.; Hagen, P. C.; Hansen, L. M.; Schwarz, R.; Bracht, T. K.; Schimpf, C.; da Silva, S. F. C.; Walther, P. Controlling the Photon Number Coherence of Solid-state Quantum Light Sources for Quantum Cryptography. *arXiv:2305.20017 [quant-ph]* **2023**, (accessed 05-01-2024).
(55) Joos, R.; Bauer, S.; Rupp, C.; Kolatschek, S.; Fischer, W.; Nawrath, C.; Vijayan, P.; Sittig, R.; Jetter, M.; Portalupi, S. L.; Michler, P. Triggered telecom C-band single-photon source with high brightness, high indistinguishability and sub-GHz spectral linewidth. *arXiv:2310.20647* **2023**. (accessed 05-01-2024)
(56) Bracht, T. K.; Cosacchi, M.; Seidelmann, T.; Cygorek, M.; Vagov, A.; Axt, V. M.; Heindel, T.; Reiter, D. E. Swing-up of quantum emitter population using detuned pulses. *PRX Quantum* **2021**, *2*, 040354.

NOTE ADDED IN PROOF

Note added in proof: During the review process of our manuscript, we became aware of related work by Joos et al.,[55] reporting experiments on the generation of indistinguishable QD telecom C-band photons using phonon-assisted excitation as well as the swing-up of quantum emitter population scheme.[56]

https://doi.org/10.1021/acsphotonics.3c00973
ACS Photonics 2024, 11, 339−347